Available online at www.sciencedirect.com

ScienceDirect

Procedia Computer Science 100 (2016) 644 – 651

Procedia Computer Science

Conference on ENTERprise Information Systems / International Conference on Project MANagement / Conference on Health and Social Care Information Systems and Technologies, CENTERIS / ProjMAN / HCist 2016, October 5-7, 2016

Mathematical models for optimal Volumetric Modulated Arc Therapy (VMAT) treatment planning

Pınar Dursun*, Z. Caner Taşkın, İ. Kuban Altınel

Department of Industrial Engineering, Boğaziçi University, Bebek, İstanbul 34342, Turkey

Abstract

Volumetric Modulated Arc Therapy (VMAT) is an external radiation treatment method, during which the gantry of the linear accelerator (linac) may rotate on one or more arc and send radiation continuously. A multileaf collimator (MLC) is mounted in the linac head in order to shape the radiation beam. These properties make VMAT powerful in obtaining high conformal plans in terms of dose distribution. However, there is interdependency between apertures that are composed by the MLC, and this makes the VMAT planning hard. In this study, we present two mixed integer linear programming models and compare them with respect to their total solution times and quality.

Peer-review under responsibility of the organizing committee of CENTERIS 2016

Keywords: Radion therapy; dose distribution; VMAT; mathematical programming

1. Introduction

The aim of radiation therapy is to destroy all cancerous cells from a target area while protecting normal tissues and critical organs by sparing surrounding structures. The radiation damages the deoxyribonucleic acid (DNA) of cancer cells and makes them unable to reproduce. However, healthy cells can renew themselves because of their self-repair mechanism if they are not exposed to high amount of radiation. Hence, the success of the treatment depends on the ability to deliver the proper amount of radiation to all structures.

* Corresponding author. Tel.: +90 (212) 359 6407 / 08; fax: +90 (212) 265 1800
E-mail address: pinar.dursun@boun.edu.tr

Peer-review under responsibility of the organizing committee of CENTERIS 2016
doi:10.1016/j.procs.2016.09.206

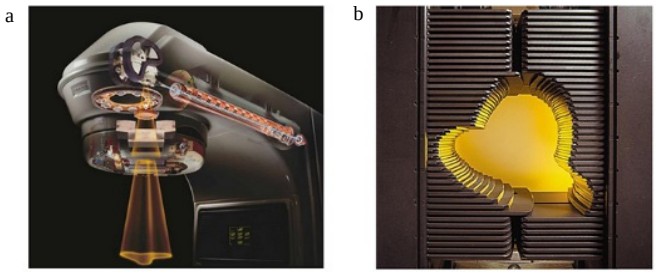

Fig. 1. (a) Linac[2]; (b) An MLC[3].

In external radiation therapy, a linear accelerator (linac) is used to generate radiation beam. The gantry of the linac is able to rotate 360 degree around the treatment couch where the patients are positioned. A beam collimator is mounted on the treatment head of the linac to shape the radiation beam. Multileaf collimators (MLCs) have been used in Intensity Modulated Radiation Therapy (IMRT) since 1990s, thus it is possible to modulate radiation intensity across a beam and conformity of the dose distribution with the planning target volume (tumor plus some margin), and normal tissue sparing are superior[1]. An MLC consists of a number of moveable leaf pairs of material that can block radiation. The radiation generated by the linac passes through this MLC and shaped beam is delivered to the patient body. In Fig. 1 a linac and an MLC are illustrated.

Volumetric Modulated Arc Therapy (VMAT), which succeeds IMRT, is a more advanced technology. The delivery time of the treatment may be about ten times shorter than the conventional IMRT, and whenever radiotherapy is well planned high conformal dose distributions with fewer monitor units (MUs) may be obtained. As the radiation therapy time decreases, risk of movement and also discomfort of the patients during treatment decreases. Resource utilization becomes more efficient, thus the number of treated patients increases. This superiority of VMAT in treatment time stems from the fact that radiation is delivered continually by rotating the gantry of the linac through one or more arcs. However, in IMRT a few discrete beam angles (generally 5-9) are used. In Fig. 2 example treatment plans for both IMRT and VMAT techniques are illustrated.

Previous studies dealing with VMAT treatment planning can be classified mainly into two categories: those are two-step approaches converting an IMRT treatment plan to VMAT plan in some fashion[6-10], and others are direct aperture optimization (DAO) methods[11-17]. In DAO studies MLC constraints and delivery time are considered simultaneously while determining a treatment plan. The studies of Gözbaşı[14], Akartunalı *et al.*[16], and Song *et al.*[17] are closely related to our research where a complete mixed integer linear program (MILP) of VMAT planning problem is given. None of these studies provide remarkable initiative to solve mathematical models optimally. They suggest heuristics to obtain only good feasible treatment plans, which are also clinically acceptable. Since the corresponding problem in VMAT treatment planning is hard, there is a lack of studies in the determination of optimal solutions. This motivates us to deal with VMAT treatment planning problem and find exact optimal treatments. In this study, we develop two MILPs for VMAT planning and compare them using a real case data set with respect to the total solution time and quality. In Section 2, we explain the mathematical models in detail. In Section 3, we report the results of the experiments briefly. Finally, we conclude the paper with Section 4.

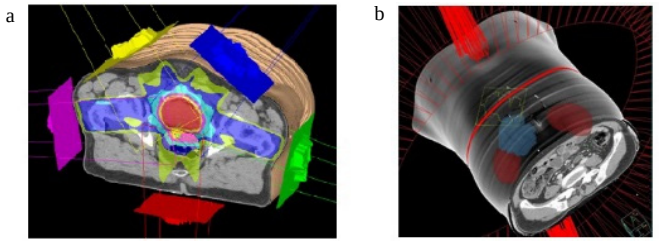

Fig. 2. (a) IMRT[4]; (b) VMAT[5].

2. Mathematical Models

We first to note that in our models we discretize continuous radiation delivery in VMAT treatment. To this end we assume that there is a large number of adjacent control points on a co-planar arc. Therefore, a complete tour on a treatment arc means that the gantry is positioned at each of these control points and delivers radiation for a certain time. Radiation delivery is ignored during movement of the gantry between consecutive angles. The planning problem determines the shape of the radiation beam and amount of radiation dose intensity at each control point. We have developed two MILP models for VMAT treatment planning problem. Each model consists of two main parts: the first part forms radiation beam shapes by satisfying mechanical necessities of the MLC and the second part determines dose intensity delivered from each control point considering the individualized radiation dose distributions. There is a relation between the dose rate of the linac and gantry rotation speed. The unit of dose rate is monitor unit (MU) per unit time, thus the dose intensity at a control point is a function of the dose rate and gantry rotation speed. As an example, if dose rate is 10 MU per second at a control point and the gantry delivers radiation for 2 seconds from this point, then dose intensity will be 20 MU. Note that a beam shape formed by the MLC is also called as aperture. In the mathematical models an aperture is represented as a binary matrix and each entry of the matrix is called beamlet. In Fig. 3 an aperture and its beamlet (binary matrix) representation are illustrated. There are partial volume constraints associated to different volumes in the models. For instance, the oncologist may decide that at least 95% of the target volume must receive radiation at least prescribed dose amount. To calculate how much volume of the target receive proper amount dose, the patient body is discretized into small cubes called voxel and absorbed dose of each voxel is calculated. The dose influence matrix D which contains the dose delivered to each voxel per unit intensity of each beamlet is used in this calculation. The D matrix is input for our optimization models and the unit of each entry is Gray per monitor unit (Gy/MU).

Our proposed models directly optimize the aperture shape and dose intensity at each control point (gantry position) by minimizing total dose intensity of all control points while satisfying all individualized dose prescriptions. In each model there are decision variables to form an aperture, namely positions of leaves of the MLC at each control point. Also, there is a decision variable per control point represents dose intensity. The differences between the proposed models MILP 1 and MILP 2 stems from the definition of the decision variables related to MLC leaves. As a result, the constraints related to the MLC are also different. In the MILP 2 we use similar decision variables as in Gözbaşı[14] to define position of leaves, however they are new in MILP 1 and firstly proposed to the literature. Similar to the study of Romeijn *et al.*[18], we construct the partial-volume constraints using the approach called Conditional Value At Risk (CVAR). Using this approach we are able to construct partial-volume constraints using only continuous variables. In the MILP model proposed by Gözbasi[14], CVAR approach is also utilized. There are similarities between our MILP 2 and his model. However, there is an additional binary variable per each beamlet and extra constraints in MILP 2. Also, there is small difference in definition of the leaves' positions (he uses corner of a beamlet as a position, thus the left and right leaf may be same value). Lastly, in MILP 2 there is a constraint per each row to prevent overlapping. Our models do not only try to find a feasible treatment, but also it tries find the treatment with minimum total dose intensity. However, maximizing the size of the target volume that receive at least prescribed amount of radiation[16], minimizing the linear summation of underdose of target volume and/or overdose of OAR[16,17], and minimizing weighted sum of the average dose on OARs[14] are some of the objective functions used in the previous studies.

In both models we assume that there is a single co-planar treatment arc (namely the gantry completes only one tour around the patient) and speed of the gantry during rotation is constant. There are 180 equally spaced control points with 2-degree spacing, which is a good approximation of the continuous delivery. At each control point the linac delivers radiation for same amount of time. It is also assumed that the MLC must satisfy consecutive ones property and efficiency constraints related to MLC leaf motion during the rotation. There is a limitation in the motion of the leaves between consecutive angles, which depends on gantry rotation speed. The MLC allows interdigitation of the consecutive rows, and connectedness is not necessary. These mechanical properties of different MLCs are explained by Gören and Taşkın[19] in detail. During rotation, intensity can change between two consecutive

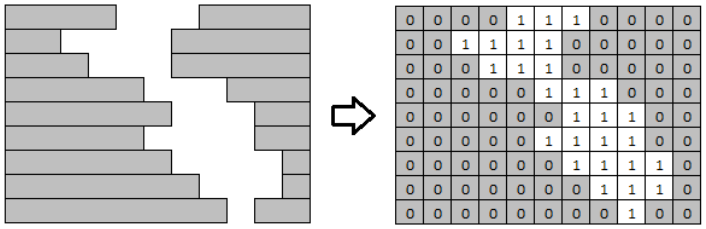

Fig. 3. An aperture and its beamlet representation including *z* variable value

control points without any limit in variation. The only necessity is that it must be within significant limits. (Because the dose rate of the linac may change during rotation). For now, we assume that there are two structures: a target and an organ at risk (OAR). However, the formulations can be modified easily by changing the parameters of additional structures. Common parameters and decision variables, and additional variables of both models are given in Table 1 and Table 2, respectively.

Table 1. Common parameters and decision variables of the MILPs.

Parameter	Definition	Parameter	Definition
I	The index set of the MLC rows (I=1,..., m)	D^k_{ijv}	Dose influence matrix (in units of Gy/MU)
J	The index set of the MLC columns (J=0,...,n+1); 0 and n+1 are home positions of left and right leaf,respectively	δ	The maximum leaf motion speed (in terms of beamlet) between two consecutive control points
V_t	Set of voxels in target volume	α_t	The minimum ratio of voxels in target that receive radiation dose at least prescribed dose
V_o	Set of voxels in OAR		
V	Set of all voxels, $V = V_t \cup V_o$	α_o	The minimum ratio of voxels in OAR that receive radiation at most tolerance dose
K	The index set of control points (gantry positions)		
L_t	Lower bound for absorbed radiation dose (in units of Gy) for target	L_{mu}	Lower bound of dose intensity (in units of MU)
		U_{mu}	Upper bound of dose intensity (in units of MU)
U_t	Upper bound for absorbed radiation dose (in units of Gy) for target	d'	Prescribed dose for target (in units of Gy)
		U_o	Tolerance dose for OAR (in units of Gy)
Variable	Definition	Variable	Definition
z^k_{ij}	Binary variable, it is set to 1 if a beamlet is within the left and right leaves of row i at control point k, 0 o.w.	ξ_t	Continuous variable stands for the $((1-\alpha_t)/\lvert V_t\rvert)$th target voxel receiving the lowest radiation dose
mu^k	Radiation dose intensity (MU) at control point k	ξ_o	Continuous variable stands for the $((1-\alpha_o)/\lvert V_o\rvert)$th target voxel receiving the highest radiation dose
a^k_{ij}	Continuous variable used for linearization	at	Artificial variable for target voxels
d_v	Total absorbed radiation dose of voxel v	Ao	Artificial variable for OAR voxels

Table 2. Additional decision variables of the MILP 1 and the MILP 2.

MILP 1		MILP 2	
Variable	Definition	Variable	Definition
l_{ik}	Positive integer variable, represents the position of the left leaf, last (rightmost) closed beamlet on the left side of row i at control point k	l^k_{ij}	Binary variable, related to the left leaf; it is set to 1 if the last (rightmost) closed beamlet of row i is j at control point k
r_{ik}	Positive integer variable, represents the position of the right leaf, first (leftmost) closed beamlet on the right side of row i at control point k	r^k_{ij}	Binary variable, related to the right leaf; it is set to 1 if the first (leftmost) closed beamlet of row i is j at control point k

Our first model (MILP 1) is as follows:

$$\min \sum_{k\in K} mu^k \tag{1}$$

s.t.

$$r_{ik} - l_{ik} \geq 1 \qquad i=1,\ldots,m;\ k=1,\ldots,|K| \tag{2}$$

$$l_{i(k+1)} - l_{ik} \leq \delta \qquad i=1,\ldots,m;\ k=1,\ldots,|K|-1 \tag{3}$$

$$l_{ik} - l_{i(k+1)} \leq \delta \qquad i=1,\ldots,m;\ k=1,\ldots,|K|-1 \tag{4}$$

$$r_{i(k+1)} - r_{ik} \leq \delta \qquad i=1,\ldots,m;\ k=1,\ldots,|K|-1 \tag{5}$$

$$r_{ik} - r_{i(k+1)} \leq \delta \qquad i=1,\ldots,m;\ k=1,\ldots,|K|-1 \tag{6}$$

$$r_{ik} - jz_{ij}^k \geq 1 \qquad i=1,\ldots,m;\ j=1,\ldots,n;\ k=1,\ldots,|K| \tag{7}$$

$$(n+1-j)z_{ij}^k + l_{ik} \leq n \qquad i=1,\ldots,m;\ j=1,\ldots,n;\ k=1,\ldots,|K| \tag{8}$$

$$r_{ik} - l_{ik} - \sum_{j=1}^{n} z_{ij}^k = 1 \qquad i=1,\ldots,m;\ k=1,\ldots,|K| \tag{9}$$

$$l_{ik} \leq n \qquad i=1,\ldots,m;\ k=1,\ldots,|K| \tag{10}$$

$$1 \leq r_{ik} \leq n+1 \qquad i=1,\ldots,m;\ k=1,\ldots,|K| \tag{11}$$

$$d_v - \sum_{k=1}^{|K|}\sum_{i=1}^{m}\sum_{j=1}^{n} D_{ijv}^k a_{ij}^k = 0 \qquad v\in V \tag{12}$$

$$a_{ij}^k \leq U_{mu} z_{ij}^k \qquad i=1,\ldots,m;\ j=1,\ldots,n;\ k=1,\ldots,|K| \tag{13}$$

$$a_{ij}^k \geq mu^k - U_{mu}(1-z_{ij}^k) \qquad i=1,\ldots,m;\ j=1,\ldots,n;\ k=1,\ldots,|K| \tag{14}$$

$$a_{ij}^k \leq mu^k \qquad i=1,\ldots,m;\ j=1,\ldots,n;\ k=1,\ldots,|K| \tag{15}$$

$$\xi_t - \frac{1}{(1-\alpha_t)|V_t|}\sum_{v\in V_t} at_v \geq d' \tag{16}$$

$$at_v \geq \xi_t - d_v \qquad v\in V_t \tag{17}$$

$$\xi_o + \frac{1}{(1-\alpha_o)|V_o|}\sum_{v\in V_o} ao_v \leq U_o \tag{18}$$

$$ao_v \geq d_v - \xi_o \qquad v\in V_o \tag{19}$$

$$d_v \geq L_t \qquad v\in V_t \tag{20}$$

$$d_v \leq U_t \qquad v\in V_t \tag{21}$$

$$mu^k \geq L_{mu} \qquad k=1,\ldots,|K| \tag{22}$$

$$mu^k \leq U_{mu} \qquad k=1,\ldots,|K| \tag{23}$$

$$l\in \mathbb{Z}_+^{m\times|K|}; r\in \mathbb{Z}_+^{m\times|K|} \tag{24}$$

$$z\in\{0,1\}^{m\times n\times|K|};\ d\in\mathbb{R}_+^{|V|};\ mu\in\mathbb{R}_+^{|K|};\ a\in\mathbb{R}_+^{m\times n\times|K|} \tag{25}$$

$$\xi_t\ urs;\ \xi_o\ urs;\ at\in\mathbb{R}_+^{|V_t|};\ ao\in\mathbb{R}_+^{|V_o|}. \tag{26}$$

The objective function (1) minimizes the sum of dose intensities at all control points. Constraints (2)-(11) are related to the mechanical restrictions of the MLC and yield a feasible aperture for each control point. For a given row the left leaf must not overlap with the right leaf and this is ensured by (2). Constraints (3)-(6) are for limiting the leaf motion: any leaf cannot move more than δ beamlets between two consecutive angles. The open beamlets for a given row must be consecutive and must be between the left and right leaves. This consecutive ones property for each row is ensured by constraints (7)-(9). By (12) the amount of radiation absorbed by voxel *v* is calculated. This constraint is linearized using the technique proposed by Glover[20] by means of constraints (13)-(15). Clinical requirements of treatment are forced by the constraint (16)-(19). Constraints (16) and (17) make the average dose of the $(1-\alpha_t)|V_t|$ voxels receiving the lowest doses in the target, namely the *lower mean tail dose at level* α_t is at least the prescription dose. When these constraints are satisfied at least $\alpha_t|V_t|$ target voxels absorb radiation more than or equal to the prescribed amount $d^{'}$. Similarly, (18) and (19) guarantee that the average dose of the $(1-\alpha_o)|V_o|$ voxels receiving the highest doses in the OAR, namely the *upper mean tail dose at level* α_o is at most the tolerance dose limit. Then, at least $\alpha_o|V_o|$ OAR voxels absorb radiation less than or equal to the tolerance dose amount. The limits of the left and right leaves' positions, the absorbed radiation dose amount for target voxels, and the dose intensity at each control point are given in the constraints (10)-(11), (20)-(21), and (22)-(23), respectively. Constraints (24)-(26) is for variable definitions. Our second model (MILP 2) is as follows:

$$\min \sum_{k\in K} mu^k$$

$$\text{s.t.} \quad \sum_{j=0}^{n} l_{ij}^k = 1 \qquad i=1,\ldots,m;\ k=1,\ldots,|K| \tag{27}$$

$$\sum_{j=1}^{n+1} r_{ij}^k = 1 \qquad i=1,\ldots,m;\ k=1,\ldots,|K| \tag{28}$$

$$\sum_{p=0}^{j} r_{i(p+1)}^k - \sum_{p=0}^{j} l_{ip}^k \le 0 \qquad i=1,\ldots,m;\ j=0,\ldots,n;\ k=1,\ldots,|K| \tag{29}$$

$$l_{ij}^{k+1} - \sum_{p=\max(0,\,j-\delta)}^{\min(n,\,j+\delta)} l_{ip}^k \le 0 \qquad i=1,\ldots,m;\ j=0,\ldots,n;\ k=1,\ldots,|K|-1 \tag{30}$$

$$r_{ij}^{k+1} - \sum_{p=\max(1,\,j-\delta)}^{\min(n+1,\,j+\delta)} r_{ip}^k \le 0 \qquad i=1,\ldots,m;\ j=1,\ldots,n+1;\ k=1,\ldots,|K|-1 \tag{31}$$

$$z_{ij}^k - \sum_{p=0}^{j-1} l_{ip}^k + \sum_{p=1}^{j} r_{ip}^k = 0 \qquad i=1,\ldots,m;\ j=1,\ldots,n;\ k=1,\ldots,|K| \tag{32}$$

$$l \in \{0,1\}^{m\times(n+1)\times|K|};\ r \in \{0,1\}^{m\times(n+1)\times|K|} \tag{33}$$

(12) - (23); (25); (26).

In this model the decision variables associated with the positions of the leaves are binary. Constraint (27) guarantee that there is only one rightmost closed beamlet of the left leaf in a row. Similar constraint for right leaf is given in (28). Overlapping of leaf pairs is prevented by (29). Leaf motion between consecutive control points is limited by (30) and (31). The consecutive ones property is satisfied (32) and for an open beamlet its corresponding *z* variable is set to 1. Finally, (33) is for modified decision variables.

3. Preliminary Results

We have implemented both MILP models in Python 2.7.11 programming language[21] and solve by Gurobi 6.5 solver[22] running on a Windows Server 2012 R2 Standard 64-bit PC with a 2.00 GHz Intel Xeon CPU, 46 GB RAM.

Gurobi solver contains efficient implementations of state-of-the-art algorithms such as branch-and-cut, cutting planes etc. to solve large scale mixed integer programming problems as our MILPs. We can direct any interested reader to Wolsey and Nemhauser[23], and Conforti *et al.*[24] for the algorithmic details. We use a real data set belonging to an anonymous prostate patient which is provided by Craft *et al.*[25]. There are 180 equispaced co-planar beams (control points), and 13 rows and 16 columns in the MLC. Also, there are 25,404 beamlets with size 1cm x 1cm, 2 target regions (PTV 68 and PTV 56), and 5 OAR regions (bladder, left femoral head, right femoral head, penile bulb, and rectum). In the preliminary experiments we only consider PTV 68. Also we unify all OARs and consider as one OAR. We reduce the size of the original data by randomly sampling the voxels from all regions. It is assumed that the number of fractions is 34 and d' is 2 Gy. We also assume that the rotation of the gantry is completed in 3 minutes, and at each control point the gantry deliver radiation for 1 second. Therefore, at each control point maximum dose intensity may be 10 MU. (Note that maximum dose rate of the linac is accepted as 600 MU/minute, thus 10 MU/s). Remaining parameters are as follows: α_o is 0.4 (%40), α_t is 0.95 (%95), U_t is 2.14 Gy, L_t is 1.9 Gy, and U_o is 1.47 Gy. For each total voxel size we generate 5 different instances from real data, and solve by the MILPs. We set time limit to 1800 seconds for each run and we use only one thread. Minimum optimality gap is set to 0.01 %. In Table 3 average performance values of only solved instances in each sample size are summarized. To give an example MILP 1 can solve four out of five instances having 660 voxels, and average CPU time and optimality gap of these four instances are given in the table.

4. Discussion and Future Direction

We try to minimize total radiation intensity in a fraction of treatment, since patients may move during treatment or there may be leakage radiation through the MLC leaves. Thus, in addition to shortening the duration of treatment, minimizing total intensity also decreases risk of damaging. However, it is also very important to find a feasible treatment plan and make possible to start treatment in a short time to prevent increasing severity of disease. As we see from preliminary results given in Table 3, the MILP 1 outperforms the MILP 2 in these two respects:

- MILP 1 can solve some of the instances (4 instances with 660 voxels, 2 instances with 880 voxels, and 1 instance with 1100 voxels), however MILP 2 cannot solve any of them within 1800 seconds. Namely, MILP 1 can find feasible treatment plans of good quality for some of the big size problems, however MILP 2 cannot give any feasible plan for any of them.
- Considering only the voxel sizes (11-220) that both MILPs solve all of 5 instances within 1800 seconds, MILP 1 is faster than MILP 2 (average CPU time is 413 seconds for MILP 1, and 680 seconds for MILP 2). Note that MILP 1 not only find good feasible treatment plan for more instances, but also solves the problem in less time.

Table 3. Preliminary results (average time and optimality gap of solved instances in each sample size).

	MILP 1			MILP 2				MILP 1			MILP 2		
Voxel Size	CPU (sec.)	GAP (%)	O/T*	CPU (sec.)	GAP (%)	O/T*	**Voxel Size**	CPU (sec.)	GAP (%)	O/T*	CPU (sec.)	GAP (%)	O/T*
11	507	0.009	5/5	716	0.006	5/5	**220**	1224	0.006	5/5	1037	0.004	5/5
22	62	0.001	5/5	378	0.003	5/5	**660**	1656	0.001	4/5	N/A	N/A	0/5
44	66	0.001	5/5	408	0.005	5/5	**880**	1800	0.079	2/5	N/A	N/A	0/5
66	501	0.034	5/5	898	0.020	5/5	**1100**	1676	0.004	1/5	N/A	N/A	0/5
88	118	0.003	5/5	646	0.003	5/5	**1301**	N/A	N/A	0/5	N/A	N/A	0/5

* Number of test instances solved / Total number of test instances

Since we set the largest allowable optimality gap to 0.01 %, it is also worth to talk about the instances that both models cannot decrease the gap below this threshold. The results are not given in instance level however there are three such instances in total (one from each sample size having 11, 66, and 220 voxels). In each one of them the MILP 2 gives slightly lower optimality gap. (Note again that CPU time and optimality gap of each individual instance is not

given, Table 3 includes only average values of the solved instances in each sample sizes). Nevertheless, we can conclude that the MILP 1, which has original decision variables associated to MLC leaves, is better than the MILP 2. It is important to note also that, both models are incapable to solve clinical size of problems to optimality. For future direction we plan to apply decomposition methods as Benders and Dantzig-Wolfe decompositions to the solution of MILP 1, and try to solve realistic clinical size problems optimally.

Acknowledgements

This research has been partially supported by the Boğaziçi University Research Fund Grant No 11520-16A03D1.

References

1. Ehrgott M, Güler Ç, Hamacher HW, Shao L. Mathematical optimization in intensity modulated radiation therapy. *Annals of Operations Research* 2010;**175(1)**:309-365.
2. http://filecache.drivetheweb.com/mr5mr_varian/154418/Inside+a+Clinac.jpg, accessed: 2016-14-06.
3. http://filecache.drivetheweb.com/mr5mr_varian/154577/MLC+-+gold.jpg, accessed: 2016-14-06.
4. http://www.simballc.org/imrt.html, accessed: 2016-14-06.
5. http://www.usa.philips.com/healthcare/product/HCNOCTN138/pinnacle3-smartarc-imrt, accessed: 2016-14-06.
6. Shepard D, Cao C, Afghan M, Earl M. An arc-sequencing algorithm for intensity modulated arc therapy. *Medical physics* 2007;**34(2)**:464-470.
7. Luan S, Wang C, Cao D, Chen DZ, Shepard DM, Cedric XY. Leaf sequencing for intensity-modulated arc therapy using graph algorithms. *Medical physics* 2008;**35(1)**:61-69.
8. Cao, D, Afghan MK, Ye J, Chen F, Shepard DM. A generalized inverse planning tool for volumetric-modulated arc therapy. *Physics in medicine and biology* 2009;**54(21)**:6725-6738.
9. Salari E, Wala J, Craft D. Exploring trade-offs between VMAT dose quality and delivery efficiency using a network optimization approach. *Physics in medicine and biology* 2012;**57(17)**:5587-5600.
10. Bzdusek K, Friberger H, Eriksson K, Hårdemark B, Robinson D, Kaus M. Development and evaluation of an efficient approach to volumetric arc therapy planning. *Medical physics* 2009;**36(6)**:2328-2339.
11. Otto K. Volumetric modulated arc therapy: IMRT in a single gantry arc. *Medical physics* 2008;**35(1)**:310-317.
12. Earl M, Shepard D, Naqvi S, Li X, Yu C. Inverse planning for intensity modulated arc therapy using direct aperture optimization. *Physics in medicine and biology* 2003;**48(8)**:1075-1089.
13. Men C, Romeijn HE, Jia X, Jiang SB. Ultrafast treatment plan optimization for volumetric modulated arc therapy (VMAT). *Medical Physics* 2010;**37(11)**:5787-5791.
14. Gözbaşı HO. Optimization approaches for planning external beam radiotherapy. Ph.D. Thesis, Georgia Institute of Technology, 2010.
15. Peng F, Jia X, Gu X, Epelman MA, Romeijn HE, Jiang SB. A new column-generation-based algorithm for VMAT treatment plan optimization. *Physics in medicine and biology* 2012;**57(14)**:4569-4588.
16. Akartunalı K, Mak-Hau V, Tran T. A unified mixed-integer programming model for simultaneous fluence weight and aperture optimization in VMAT, Tomotherapy, and Cyberknife. *Computers & Operations Research* 2015;**56**:134-150.
17. Song J, Shi Z, Sun B, Shi L. Treatment Planning for Volumetric-Modulated Arc Therapy: Model and Heuristic Algorithms. *IEEE Transactions on Automation Science and Engineering* 2015;**12(1)**:116-126.
18. Romeijn HE, Ahuja RK, Dempsey JF, Kumar A. A new linear programming approach to radiation therapy treatment planning problems. *Operations Research* 2006;**54(2)**:201-216.
19. Gören M, Taşkın ZC. A column generation approach for evaluating delivery efficiencies of collimator technologies in IMRT treatment planning. *Physics in medicine and biology* 2015;**60(5)**:1989-2004.
20. Glover F. Improved linear integer programming formulations of nonlinear integer problems. *Management Science* 1975;**22(4)**:455-460.
21. https://www.python.org/about/, accessed: 2016-14-06.
22. http://www.gurobi.com/products/gurobi-optimizer/gurobi-overview, accessed: 2016-14-06.
23. Wolsey, LA., Nemhauser GL. *Integer and combinatorial optimization*. John Wiley & Sons; 2014.
24. Conforti M, Cornuéjols G, Zambelli G. *Integer Programming*. Berlin: Springer; 2014.
25. Craft D, Bangert M, Long T, Papp D, Unkelbach J. Shared data for intensity modulated radiation therapy (IMRT) optimization research: the CORT dataset. *GigaScience* 2014;**3(1)**:1-12.